STUDY OF SLAG-METAL REACTIONS IN AN LD-LBE CONVERTER

C. Cicutti*, M. Valdez*, T. Pérez*
J. Petroni**, A Gómez**, R. Donayo**, L. Ferro**

* FUDETEC, J. Simini 250 (2804) Campana, Argentina
** SIDERAR, CC 801 (2900) San Nicolás, Argentina

ABSTRACT

Samples of slag and metal were taken from an industrial converter at different stages of the process. Chemical composition of samples was determined using standard analytical methods. The metallic emulsion present in slag samples was also separated and analysed. Size distribution and chemical analysis of the droplets were performed. A minimum FeO content in the slag was observed close to the middle of the blow. Besides, a maximum bath decarburization and phosphorus reversion were also observed at this part of the process. The influence of metallic emulsion on the global decarburization reaction was analysed and the phosphorus reaction during the process was discussed.

1. INTRODUCTION

In the converter operation, a proper control of the slag-metal reactions that take place along the process is required to guarantee successful results. An inadequate slag and metal path can promote operative problems (like slopping or lance skull formation) or unsatisfactory metallurgical results (e.g. poor dephosphorisation). Although slag and metal samples are taken at the end of the process during routine operation, the path that they follow along the blow is not completely known. The aim of the present work was to study the evolution of metal and slag composition along the process. The results obtained were applied to better understand the slag-metal reactions that take place during the blow.

2. EXPERIMENTAL WORK

2.1 Process conditions

Trials were performed at Siderar in a 200 ton industrial converter. It is an LD converter where inert gas is blown through the bottom (LBE system) [1]. Usually, low and medium carbon steels are produced for different applications, like tinplate, deep drawing steels and API grades. About 40 heats per day are processed in two converters.

A brief description of the process conditions employed during the trials and the different additions carried out along the blow are listed in Table 1. Figure 1 shows the lance height profile used during the trials, together with the points where samples were taken.

2.2 Sampling procedure

Slag and metal samples were taken from the mouth of the converter at different times from the start of the blow, see Fig 1 [2]. The sampling was carried out with the aid of a special device which enables the obtaining of slag and metal samples all at once [3], see Fig. 2. Only one sample was taken in each heat by interrupting the blow and submerging the sampler into the converter. In order to develop a more representative picture, at least five samples were taken in each sampling point.

2.3 Samples analyses

After collection, the slag samples were gently crushed in order to separate the metallic particles within them. Special care was taken with the material sampled at the beginning of the oxygen blow when the carbon content is normally high and, consequently, the metallic particles are fragile. The metallic droplets were magnetically separated from the slag to measure size distribution, oxygen and carbon content. The slag and metal composition was determined by standard methods (atomic absorption and UV spectrometry).

3. RESULTS AND DISCUSSION

3.1 Slag and metal path during the blow

The evolution of the main slag components during the blow is shown in Fig. 3. At the beginning of the process the FeO content is high, allowing lime to be dissolved into the slag. Silicon of the hot metal is oxidised during the first minutes (see Fig. 5), promoting a slight increase of SiO_2 in the slag. Due to lime and dolomite additions, the CaO content of the slag increases continuously during the first part of the blow. Also, a slight increase of MgO is noted. Near the middle of the process a decrease in the FeO content is observed, which almost coincides with the period of maximum decarburization of the bath. Towards the end of the process, the decarburization rate decreases and part of the oxygen blown is consumed to form FeO. Consequently, an increment of the slag FeO content is verified (Fig. 3).

Figure 4 shows the evolution of slag composition in a $CaO´$-$SiO_2´$-$FeO´$ ternary system. The path followed by the slag during the process is similar to that observed by other researchers [3-4]. In the same figure, the isotherms reported in the literature for this system have also been plotted [5-6]. Assuming that the temperature varies linearly from 1350 to 1650 °C along the process, the slag is, in general, above its liquidus temperature. This means that only little solid precipitation should be expected during the blow for this process conditions.

The evolution of the Si, P and Mn contents in the metal bath are plotted in Fig. 5. As was mentioned before, silicon is almost completely eliminated in the first three minutes. On the other hand, Mn and P are partially consumed in the first oxidation stage of the process, showing a reversion near the middle of the blow.

Using the metal and slag silicon contents measured along the process, mass balance calculations were performed in order to estimate the evolution of slag weight [2]. In general, the slag weight increases at the beginning of the process, reaching a plateau at about 30 % of the blow. In the last part of the process, the weight increases again up to 16 tons.

3.2 Characterisation of metallic emulsion

3.2.1 Droplet morphology

Figure 6 shows the aspect of the metallic emulsion after being separated from the slag. When inspected in more detail using a magnifying glass, cavities were found in some of the droplets, see Fig. 7. The same morphology has been previously reported by Meyer [7-8]. In general, these cavities are attributed [7] to the carbon monoxide evolution during the decarburization process. Gas bubbles can nucleate in the droplet and, in some cases, the reaction produce a disintegration of the metal particle. As will be discussed later, this reaction can contribute to the global decarburization process.

3.2.2 Droplet size distribution

The size of the particles ranged from 0.23 to 3.35 mm with a mean value of 1 to 2 mm. According to pilot plants experiments and industrial trials, the size distribution of the droplets generated during the BOF process can be well represented using the Rosin-Rambler-Sperling (RRS) function [9-11]. In such a case, the cumulative weight percent of particles remaining on the sieve with diameter *d* is:

$$R\ (\%) = 100.\exp[-(d/d')^n] \quad (1)$$

where *n* and *d´* are parameters of the distribution. The value of *d´* is a measure of the sample fineness and represents the statistical droplet size for R = 36.8% cumulative weight retained. The exponent *n* is independent of the fineness but it is characteristic of the substance [9]. The values of *n* and *d´* for the collected samples were determined fitting the measured data by the least square method (see Fig. 8 as an example). The results are summarised in Table 2 showing a reasonable agreement with data reported in trials with industrial converters [8-9]. Nevertheless, results obtained in laboratory scale experiments usually present higher *d'* values [9].

3.2.2 Carbon content

Despite the fact that samples were carefully washed before chemical analysis, traces of slag could still remain stuck to the particles (specially in those cases with cavities or with a tortuous shape). The presence of slag stuck to the particles can induce errors in the determination of carbon content. Consequently, total oxygen determinations were carried out in order to correct the results, following a similar procedure to the one published elsewhere [7].

In general, the carbon content measured in the particles was below the bulk composition measured in the samples taken from the bath at the same time, see Fig. 9. A similar result has been reported in the literature [12]. The degree of decarburization of the droplets can be quantified with the following parameter:

$$\Phi_C = (C_B - C_D) / C_B \quad (2)$$

where C_D is the carbon content measured in the droplets of size d (after correction by total oxygen determinations) and C_B is the carbon content in the bulk. Figure 10 shows that the degree of decarburization of the droplets increases when their sizes decrease.

3.3 Analysis of decarburization reaction

Figure 11 shows the evolution of carbon content along the process. The three different zones usually reported in the literature [13-15] can be clearly distinguished along this curve:

i) Initial period: The decarburization rate increases with time
ii) Main period: Decarburization rate is approximately constant.
iii) Final phase: The decarburization rate decreases with time

During the second period the decarburization rate is mostly controlled by the oxygen supply. Considering an oxygen flowrate of 620 m^3/min (Table 1) and a $CO_2/(CO+CO_2)$ ratio of 0.10 [15] , the theoretical decarburization rate can be estimated:

$$dC/dt = 0.909\ x\ 100\ x\ \frac{620\ m^3/min}{0.0224\ m^3/mol}\ x\ 24\ grs/mol\ x\ \frac{10^{-6}\ ton/gr}{200\ ton} = 0.30\ \%/min \qquad (3)$$

which is in close agreement with the one obtained experimentally (Fig. 11) and the values reported in the literature [14].

When the carbon content is reduced below a certain level, the decarburization process begins to be controlled by carbon diffusion. This critical carbon content depends on different variables, for example the oxygen flow rate. Using previously reported results [15] a critical carbon content around 0.35 % could be expected for the process conditions present in these trials (see Table 1). This value is consistent with the results showed in Fig. 11.

Figure 9 shows the carbon content measured in the metallic droplets separated from the slag. It is clear that the particles are much more decarburized than the bulk metal, indicating that the metallic emulsion plays an important role in the global decarburization reaction. In the same figure, the carbon content in equilibrium with the slag was calculated. For these calculations the following reaction was considered:

$$FeO + [C] = Fe + (CO)g \qquad (4)$$

$$K_C = a_{Fe}.p_{CO} / fc.[\%C].a_{FeO} \qquad (5)$$

Taking into account that $a_{Fe} = 1$ and assuming a pressure of 1 atm in the carbon monoxide bubbles, the following expression was obtained:

$$[\%C] = 1/a_{FeO}.fc.K_C \qquad (6)$$

Where the equilibrium constant value was taken form the literature [16]:

$$\log K_C = 5.096 - 5730/T \qquad (7)$$

It was assumed that slag temperature changes linearly along the process from 1350 to 1650 °C. The activity of FeO was evaluated using the regular solution model developed by Ban-Ya [17-18] and the results published by Suito and Inoue [19]. In both cases, the calculated equilibrium carbon content is lower than the value measured in the droplets, see Fig. 12. This result suggests that the droplets are partially decarburized during their contact with the slag. Full decarburization is not achieved, probably due to the short residence time, which is around 0.25 to 150 seconds, being 60 seconds the most probable value [20].

The contribution of the metallic emulsion to the global decarburization reaction was estimated by coupling the decarburization measured in the droplets with the mass of metal emulsified during the process. Calculations were carried out using both the emulsified mass measured in this work and theoretical expressions developed in the literature [15]. Preliminary results show that about 20-50 % of the total decarburization takes place in the droplets.

3.4 Analysis of phosphorus reaction

In most cases, the exchange of phosphorus between metal and slag is described by the following reaction:

$$\underline{P} + 5/2\ \underline{O} = (PO_{5/2}) \quad (8)$$

where $\underline{P}$ and $\underline{O}$ are the phosphorus and oxygen dissolved in the melt. Assuming that the reaction is mainly controlled by phosphorus diffusion in the metal and that thermodynamic equilibrium is achieved at the slag-metal interface, the following equation is proposed:

$$d\underline{P}_B/dt = -M_P\ (\underline{P}_B - \underline{P}_i) \quad (9)$$

where $\underline{P}_B$ is the phosphorus content in the bulk metal, $\underline{P}_i$ the concentration at the slag-metal interface and M_P is the mass transfer coefficient. Under equilibrium conditions, the concentration at the interface can be calculated with the following expression:

$$\underline{P}_i = [\gamma PO_{5/2}\ XPO_{5/2}] / [(f_P.K_P).a_O{}^{5/2}] \quad (10)$$

where $\gamma PO_{5/2}$ is the activity coefficient of $PO_{5/2}$, X_i is the molar fraction of the *i* component in the slag and K_P is the equilibrium constant of the reaction (8). The oxygen activity can be estimated from the following reaction:

$$\underline{Fe} + \underline{O} = (FeO) \quad (11)$$

Under equilibrium conditions, the following equation can be used to obtain the oxygen activity:

$$a_O = \gamma FeO\ XFeO / K_F \quad (12)$$

where γFeO is the activity coefficient of FeO in the slag and K_F is the equilibrium constant. Both coefficients ($\gamma PO_{5/2}$ and γFeO) were calculated using the formalism developed by Ban-Ya [17-18]:

$$RT \ln \gamma_i = \Sigma_j\ \alpha_{ij}\ X_j^2 + \Sigma_j\ \Sigma_k\ (\alpha_{ij} + \alpha_{ik} - \alpha_{jk})\ X_j.X_k + I' \quad (13)$$

Using the slag composition data obtained along the process (see 3.1) and assuming a linear variation of temperature during the blow, the phosphorus content at the interface was calculated at each stage with equations (10) to (13).

Coupling equation (9) with a mass balance of the slag-metal system, the phosphorus content of the bulk metal can be estimated. The mass transfer coefficient was varied until a reasonable agreement was found between calculated and measured data. Two different approaches were developed. First, a constant mass transfer coefficient was used. Then a coefficient that varies with the amount of gas generated in the process was employed [21]. The results are summarised in Fig. 13 where it can be observed that the calculated values follow the trend shown by the measured values. In this particular case, the decrease of FeO content at the

middle of the blow causes a reduction of the oxygen activity at the interface, increasing the equilibrium phosphorus content, see equation (10). When the value of $\underline{P}_i$ becomes higher than $\underline{P}_B$, phosphorus reversion takes place. Close to the end of the blow the slag FeO content increases again, enabling the phosphorus in the metal to be reduced. Normally, the post-stirring operation after the end of the blow further contributes to the lowering of the phosphorus content [1].

4. CONCLUSIONS

Samples of slag and metal were taken from an industrial converter at different stages of the process. As a result of the analyses carried out on these samples the following findings can be highlighted:

- A significant change of slag composition is verified along the process. While at the beginning of the blow the FeO content is relatively high, it drops at the middle of the process. A new increase in the FeO content is observed near the end of the blow. Hot metal silicon is oxidised during the first minutes, promoting a slight increase of SiO_2 in the slag. Due to additions of lime and dolomite, the CaO content of the slag increases continuously during the first half of the blow.

- The evolution of carbon content in the bath shows three well defined zones. At the beginning the decarburization rate is low due to oxygen consumption in reactions with other elements. At the middle of the process the decarburization rate reaches a maximum. Calculations show that almost all the oxygen blown is consumed in the decarburization reaction.

- Metallic particles found in the slag were separated and analysed. Similarly to previously reported studies, the size of the metallic particles follow a Rosin-Rambler-Sperling distribution. The coefficients obtained using this distribution are close to those reported in the literature for trials in industrial converters. In general, metal droplets were more decarburised than samples taken from the bath, indicating that they have an active participation in the decarburization of the metal. The degree of decarburization is larger in the smaller droplets. However, the carbon content of the droplets is above the expected equilibrium value. This might be attributable to an insufficient residence time in the slag. Preliminary calculations indicate that about 20-50 % of the global decarburization can take place in the metallic emulsion present in the slag.

- Although at the beginning of the process the phosphorus content in the melt is reduced, a reversion is verified at the middle of the blow. This increase in the bath phosphorus content coincides with the decrease in the slag FeO content. Calculations have shown that the reduction in the slag FeO content promotes an increase of the phosphorus content at the slag-metal interface, inducing the reverse reaction. Close to the end of the blow the FeO content increases again, enabling phosphorus in metal to be reduced. Normally the post-stirring operation after the end of the blow also contributes to the lowering of the phosphorus content.

nd European Oxygen Steelmaking Congress, Oct. 1997, p. 69-78.

2. C. Cicutti, M. Valdez, T. Pérez, R. Donayo, A. Gómez, J. Petroni, “Study of slag and metal evolution in the converter”, 12º IAS Steelmaking Seminar, Argentina, 1999, p. 629-638.
3. A. van Horn, J. van Konynenburg, P.J. Kreyger, “Evolution of slag composition and weight during the blow” Mc Master Symposium Nº7: The role of slags in Basic Oxygen Steelmaking, May 1976, p. 2.1-25.
4. P.Kreijer, R.Boom, “Slag formation in large scale BOF steelmaking”, Canadian Metallurgical Quarterly, 1982, Vol. 21, Nº4, p. 339-345.
5. H. Margot-Marette, P. Riboud, “Fusibilité et cristallisation des laitiers basiques peu phosphatés d´aciérie”, Revue de Metallurgie, 1964, Vol. 61, p.709-716.
6. K. Mills, B. Keene, “Physical properties of BOS slags”, International materials Review, 1987, Vol.32, Nº 1-2, p. 1-120.
7. H. Meyer, “Oxygen Steelmaking: Its control and future”, JISI, June 1969, p. 781-789.
8. H. Meyer, W. Porter, G. Smith, J. Szekely, “Slag-metal emulsions and their importance in BOF Steelmaking”, JISI, July 1968, p. 35-42.
9. S. Koria, K. Lange, “A new approach to investigate the drop size distribution in Basic Oxygen Steelmaking”, Metall Trans. B, Vol.15B, March 1984, p.109-116.
10. S. Koria, K. Lange, “Effect of top blowing parameters on drop size distribution in BOF ., Vol.55, 1984, Nº 12, p.581-584.
11. N. Standish, Q. He, “Drop generation due to impinging jet and the effect of botton blowing in the steelmaking vessel”, ISIJ International, 1989, Vol. 29, Nº6, p.455-461.
12. A. Chaterjee, N. Lindfors, J. Wester, “Proces metallurgy of LD steelmaking”, Ironmaking and Steelmaking, 1976, N° 1, p. 21-32.
13. M. Ichinoe, S. Yamamoto, Y. Nagano, K. Miyamura, K. Yamaguchi, M. Tezuka, “A study on decarburization reactions in Basic Oxygen Furnace”, Proceedings ICSTIS, Suppl. Trans ISIJ, 1971, Vol. 11, p. 232-235.
14. E. Turkdogan, “Fundamentals of Steelmaking”, The Institute of materials, 1996.
15. B. Deo, R.Boom, “Fundamentals of Steelmaking metallurgy”, Prenctice Hall International, 1993.
16. E. Turkdogan, "Controlling effect of iron oxide in slag on BOF and Q-BOP steelmaking reactions", ISS Alex Mc Lean Symposium Proceedings, 1998, p.29-39.
17. R. Nagabayashi, M. Hino, S. Ban-ya, “Mathematical expression of phosphorus distribution in steelmaking process by quadratic formalism”, ISIJ International, 1989, Vol. 29, Nº 2, p. 140-147.

18. S. Ban-Ya, “Mathematical expressions of slag-metal reactions in steelmaking process by quadratic formalism based on the regular solution”, ISIJ International, 1993, Vol. 33, p. 2-11.
19. H. Suito, R. Inoue, “Thermodynamic assessment of hot metal and steel dephosphorization with MnO containing BOF slags”, ISIJ International, 1995, Vol. 35, Nº 3, p. 258-265.
20. L. He, N. Standish, “A model study of residence time of metal droplets in the slag in BOF steelmaking”, ISIJ International, 1990, Vol. 30, p. 356-361.
21. H. Gaye, J. Grosjean, “Metallurgical reactions in the LBE process”, ISS Steelmaking Proceedings, 1982, p. 202-210.

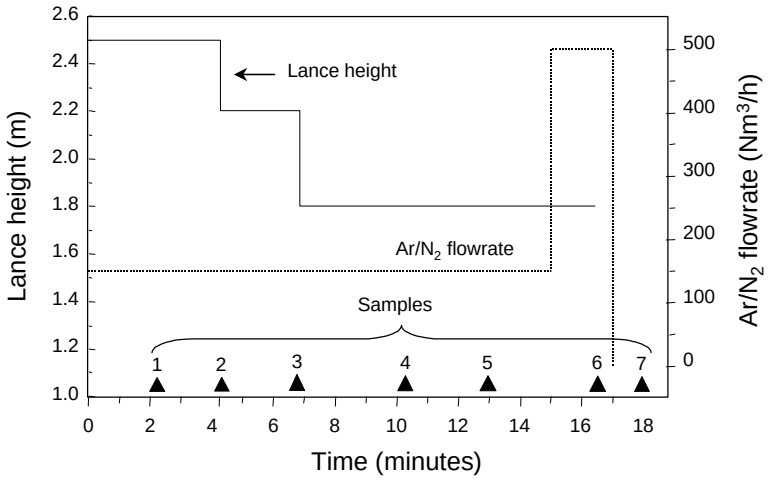

Fig. 1 Lance height along the process and sampling points

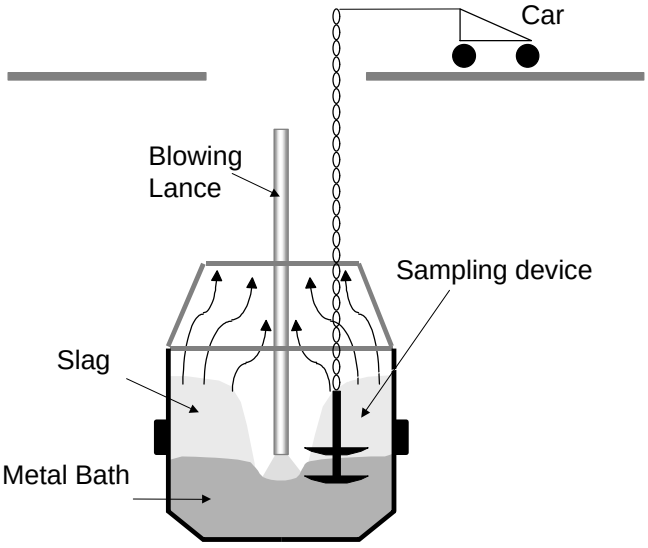

Fig. 2 Sampling procedure used in the converter

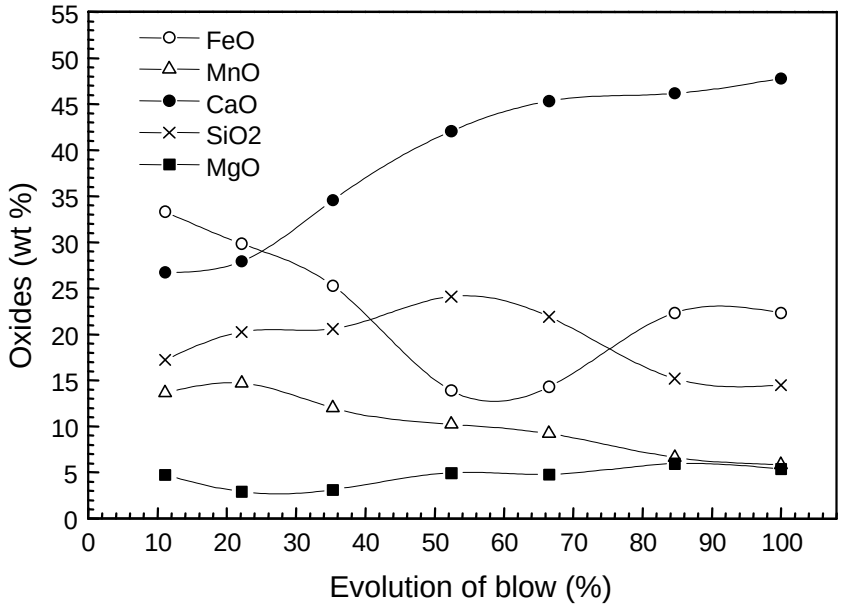

Fig. 3 Evolution of slag composition during the process

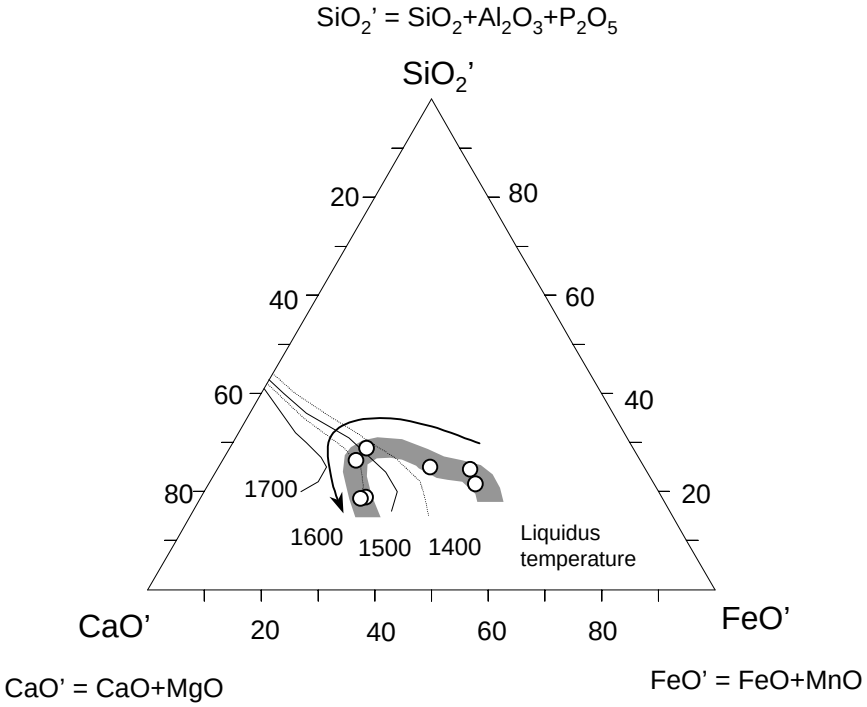

Fig. 4 Slag path in a CaO'-FeO'-SiO_2' ternary system

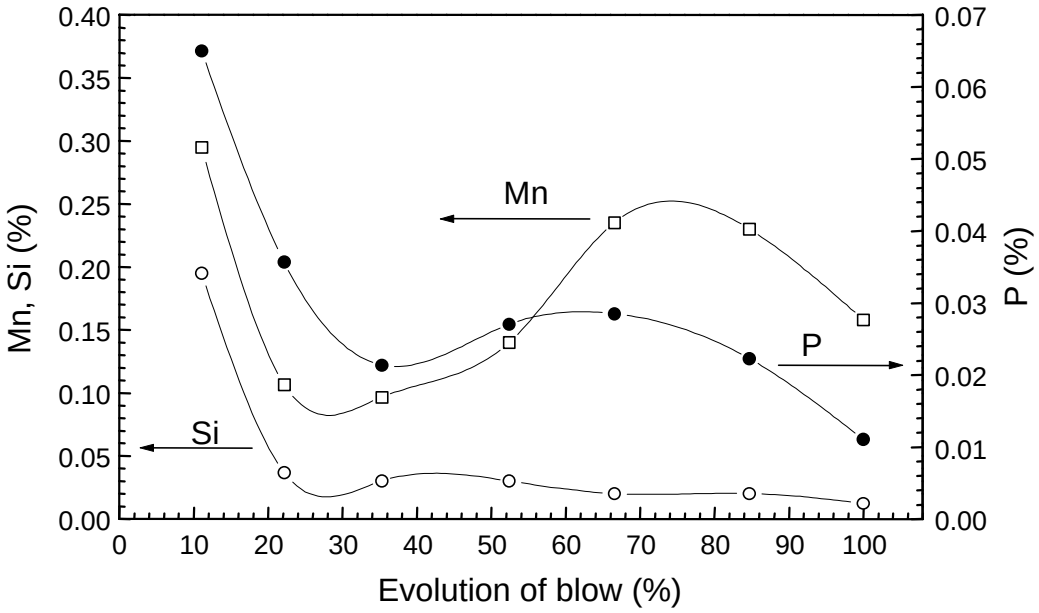

Fig. 5 Evolution of melt composition during the process

Fig. 6 General aspect of the particles separated from slag

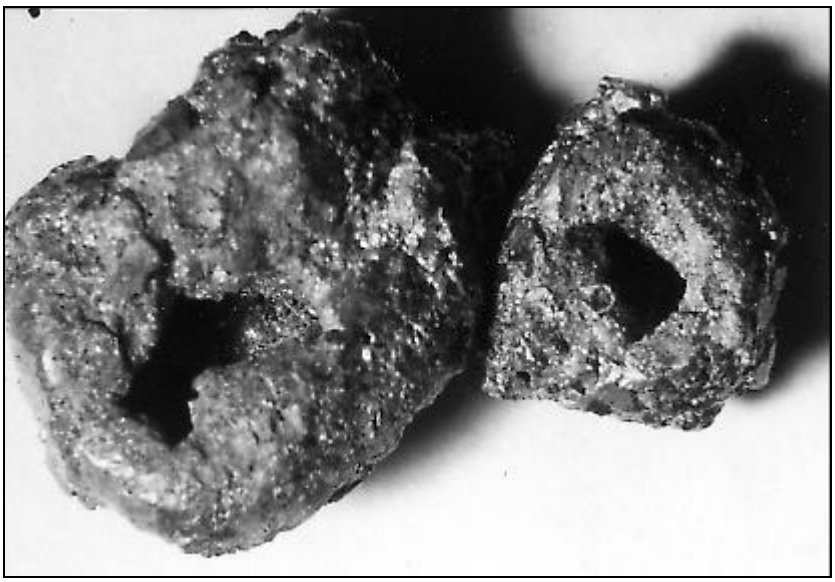

Fig. 7 Detail of some of the particles showing cavities

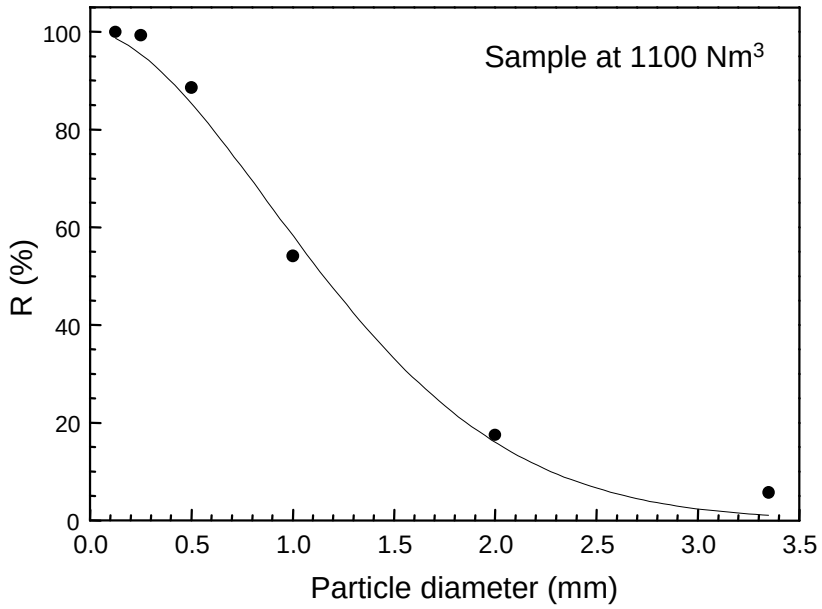

Fig. 8 Fitting of RRS distribution in one of the samples (1100 Nm^3)

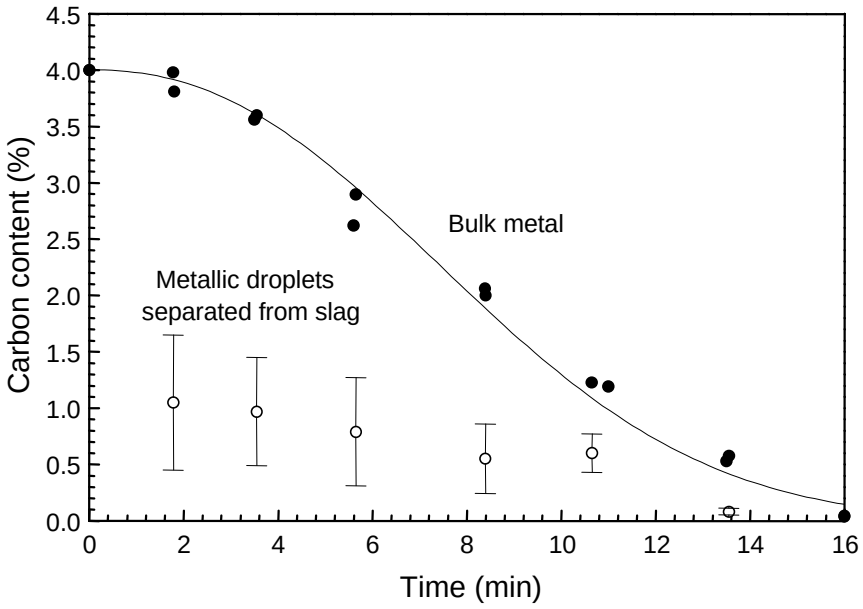

Fig. 9 Evolution of carbon content in the melt and in the metallic particles separated from the slag.

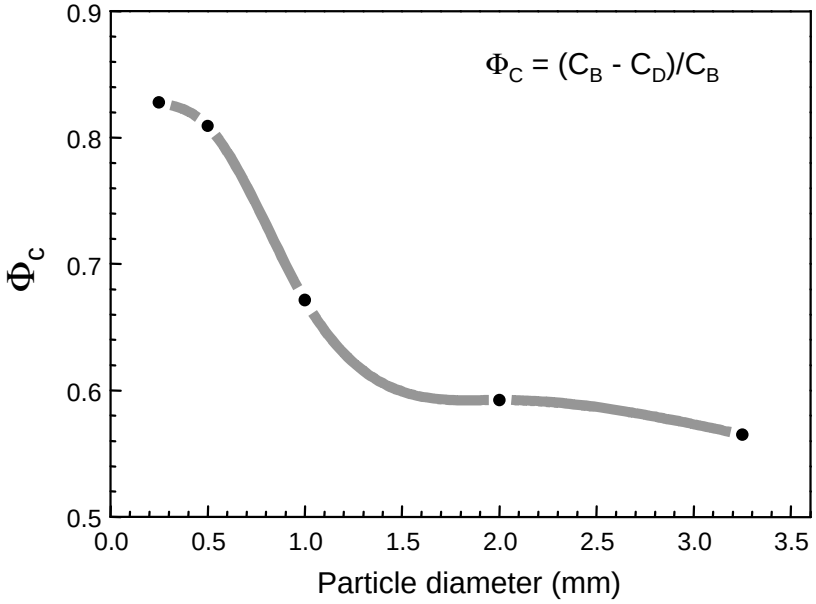

Fig. 10 Influence of the droplet size on the degree of decarburization, see equation (2)

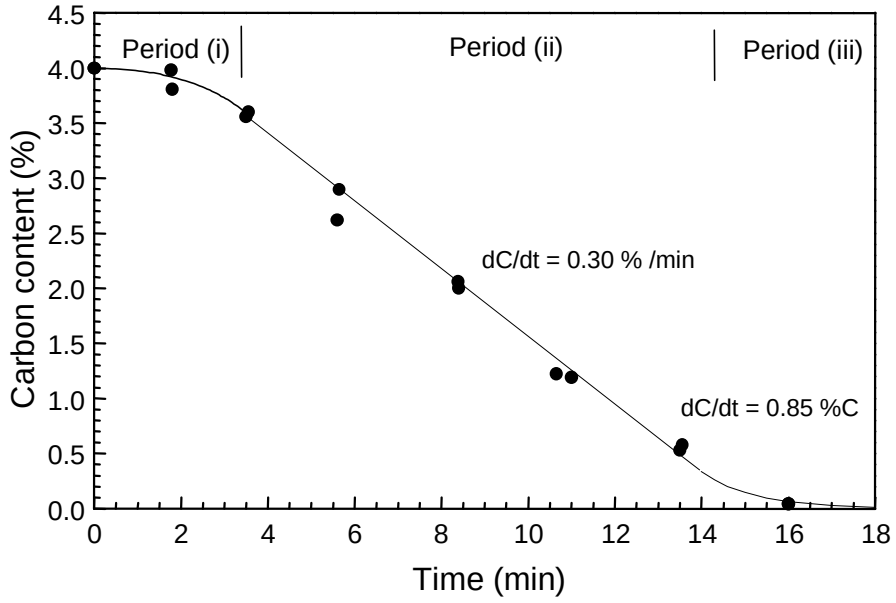

Fig. 11 Evolution of carbon content during the process.

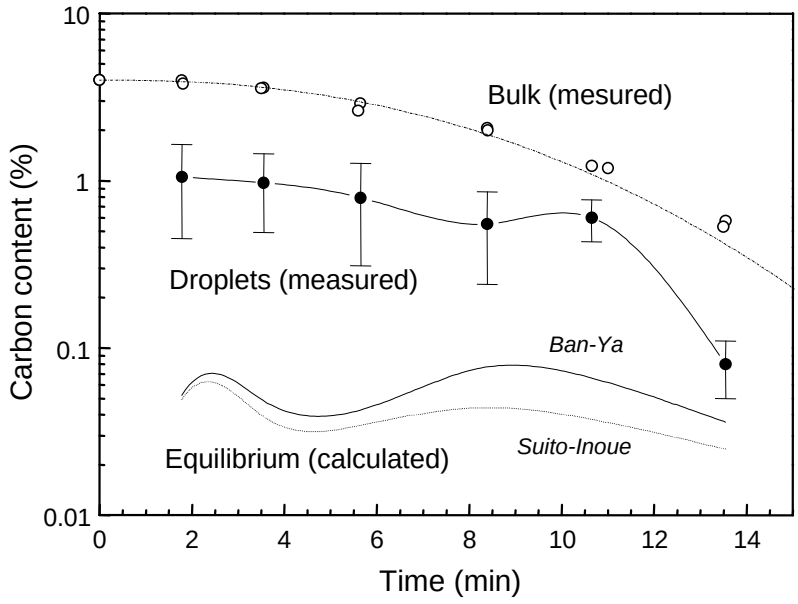

Fig. 12 Evolution of carbon content measured in the droplets and carbon in equilibrium with the slag, calculated with two different models

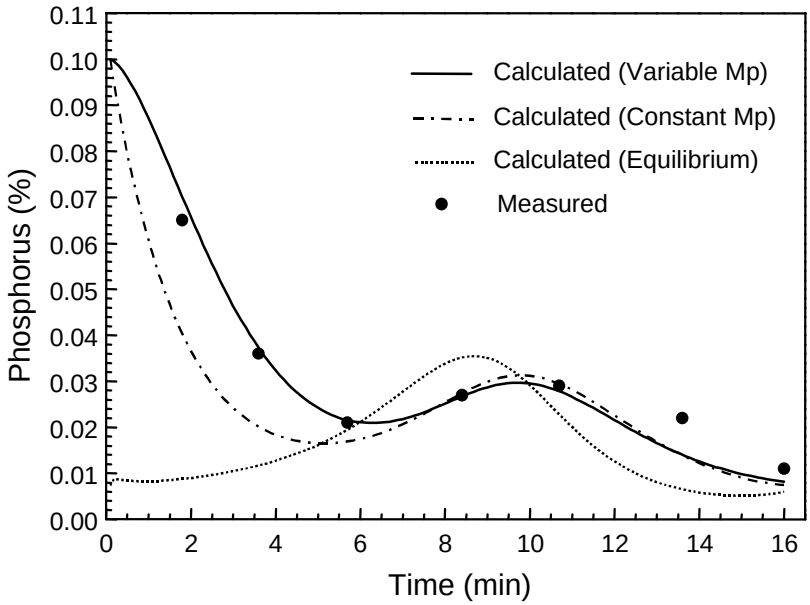

Fig. 13 Evolution of slag and metal phosphorus content during the process. Comparison between measured and calculated results.

Table 1 Additions carried out during the blow and main process conditions

Lime	1000 kg before starting the blow 6600 kg in the first half of the process.
Dolomite	2800 kg
Cuarcite	800 kg
Iron ore	1900 kg
Oxygen blow	620 m^3/min. Six holes lance.
Inert gas (Ar/N_2)	150-500 m^3/h blown trough the bottom
Lance height	2.5 m / 2.2 m / 1.8 m (see Fig. 1)

Table 2 RRS parameters obtained after fitting the experimental data

O_2 (Nm^3)	d´	n
1100	1.418	1.764
2200	1.232	1.700
3500	2.005	1.551
5200	1.484	1.828
6600	1.493	1.581
8400	2.609	1.466